

# The Effect of Voltage Change on the Heat Affected Zone in Electric Spark Process

Jabbar k. Abbas 1\*, Shukry. H. Aghdeab2

<sup>1</sup>Department of Scholarships and Cultural Relations.  
Baghdad / Ministry of Higher Education and Scientific Research.

<sup>2</sup>Nanotechnology and Advanced Materials Research Center (NAMRC), University of Technology  
Baghdad, Iraq

\*Corresponding Author: [jabbarkadhim14@gmail.com](mailto:jabbarkadhim14@gmail.com)

## ABSTRACT:

Heat-affected zone (HAZ) is a type of highly active zone that may be created by welding in AISI 444 stainless steel buildings, by utilizing machining modeling of an AISI 444 stainless steel alloy under complex heat operation, but the ductility and modeling techniques for HAZ in numerical simulations are unclear. The problem is resolved by combining experimental and numerical work on machining modeling of a specific alloy under complex heat operation, which is useful for predicting the general behavior of structures. The use of the Electro Discharge Machining (EDM) process machine to produce carefully defined heat treatments with high peak temperatures and heating rates using precisely defined methods also accounts for the impact of the two models, both theoretical and practical, on the definition of power supply voltage change, The overarching aim of this research is to gain a more universal comprehension of ductile machining modeling of machining-related AISI 444 stainless steel alloys that are exposed to varying voltages, complex heat operation, and are representative of machining. The EDM parameters employed had an increase in HAZ due to an increase in voltage (140, 240) V, current  $I_p$  (12, 24, 50) A, pulse on time  $T_{on}$  (100, 200, 400)  $\mu\text{m}$ , and pulse off time  $T_{off}$  (3, 6.5, 12)  $\mu\text{m}$ . Tests showed that these values had a positive impact on HAZ and an increase in HAZ at the same time. However, four parameters were tested to determine the accuracy of the results: voltage (140, 240) V, current  $I_p$  (12), voltage, current and pulse rates are gradual increases with increasing voltage and current, while the current increases gradually with increasing current and pulse.

**Keywords:** Heat Affected Zone (HAZ), EDM process

## 1. INTRODUCTION

Electrical discharge machining (EDM) is an advanced manufacturing process that operates based on the thermal energy principle. This thermal energy causes material ablation, leading to significant modifications in the subsurface layers and resulting in material loss. These changes can directly influence the surface integrity of the manufactured component. Understanding these material transformations enables an early evaluation of the component's functional performance. A phase-field method-based model is employed to simulate the microstructural evolution within the heat-affected zone of steel as detailed in Reference [1]. The microstructure evolution models, utilizing heat transfer simulation data from different regions of the rim zone, enable the determination of the final heat-affected zone's location. Subsequently, the properties of the rim zone are derived by calculating phase fractions (phenyle phases) using the microstructural evolution model. These are then combined with the rim zone's characteristics to define the properties of the pure phases.

The EDM process and Pulse Electrochemical Machining (PECM) provide distinct machining capabilities for a range of materials. EDM is effective for machining electrically conductive materials above a certain threshold, though it involves some tool wear and generates heat. On the other hand, PECM faces challenges when cutting materials that are chemically soluble or tend to form a passive layer. To address these limitations, a process chain can be established where copper electrodes are first fabricated using PECM and subsequently utilized in EDM. This approach allows the electrodes to be refined through PECM, ensuring consistent machining geometry with high quality and reproducibility [2].

Functional properties provide an effective means to predict and simulate microstructure evolution, enabling the development of an inverse modeling approach for the manufacturing process. Previous studies by the authors introduced models for microstructure evolution under thermal loads, utilizing artificial initial structures and temperature gradients as high as 1106 K/s. These models were extended to predict single-discharge temperature gradients in electrical discharge machining (EDM) by enhancing an existing heat transfer model. The presented model demonstrates a high degree of accuracy in simulating the actual microstructure evolution within the heat-affected zone of an EDM-processed workpiece. Reference 4 explores the influence of geometric and energetic

heterogeneities on the surface structure and electrode geometry, along with the positioning and formation of erosion craters, in relation to discharge occurrence and location. In numerical simulations of electrical discharge machining, a multi-stage approach is employed, involving the repetitive execution of key steps: analyzing thermal processes associated with individual discharges, simulating material removal and crater formation during intervals, determining the site of subsequent discharges, and applying the transient heat conduction equation to a medium with dynamically changing physical and chemical properties due to heat conduction effect.

Some non-traditional manufacturing processes use Electrical discharge EDM as a method of machining that is commonly known as slow machining, The search for better EDM performance characteristics is being conducted to determine the most effective methods, such as enhancing the material removal rate (MRR) and lowering the tool wear rate (TWR), Several reference study [5] has been developed to address the issue of overarching factors in EDM process development, specifically the enhancement of tool design by variations in various tool materials used, with the goal of improving the performance of the EDM process. This approach involves comparing the results of different tool designs applied to different tool materials to examine the impact of these combined tool designs and materials on key performance indicators in EDM die-sinking. Modified tool designs are created by reducing machining time by 45% compared to previous generation tools using the latest tools, including MRR, TWR\_L. The MEMS industry recognizes the importance of the micro electrical discharge machining process and generally prefers the micro-die sinking process that necessitates the optical solidification of the surface of die electrodes before die-die sinking, making it a preferred method [6]. The wear phenomena and morphology of copper electrodes were investigated as part of a larger experiment to investigate these and other wear phenomena. A numerical model is constructed using the Gaussian distribution of heat flux to approximate the crater dimensions formed in the copper tool electrode (tool wear) used due to electric discharge. To model the wear of crater distribution craters with less than 30% overlap and 50 % overlap, the single discharge study's crater dimensions are applied to crater distribution craters with less than 30 % overlap and 50 % overlap for different scenarios of crater distribution craters.

Micro-EDM, or micro electrical discharge machining (micro-EDM), is a method that has been harnessed and used to design high-quality components, as well

as to monitor them, model their behavior, simulate AI-based and multi-physics models, and conduct physics experiments to improve process information. This challenge is effectively addressed using RF-based approaches, which are recognized as cost-effective and non-invasive methods for process monitoring, as recommended in [7]. The results indicate that breakup voltage and gap current are the sole factors influencing RF intensity.

Using the tool's shape and gases, the material removal rate (MRR) and surface roughness (SR) of the specimen can be measured and adjusted based on the shapes and gases present in the tool. To tackle the challenges of low MRR and poor surface integrity, a new process called DEDM or swirl assisted flushing (a new paper in Reference [8], cited in 2011) was suggested, which involves applying DEDM to remove blemishes on the surface, according to the journal, using a new low-resolution method. Swirl assisted flushing, which involves the use of tricks to work around Decay Law, can also be substantiated by microscopic investigation that validates its observable by design, Studies indicate that current and pulse-on time are the primary factors influencing machining performance., contributing approximately 53.3% and 27% of the overall impact, respectively. This allows MRR to improve significantly without a notable increase in Ra.

Machine learning-based optimization methods are employed to enhance trajectory planning for EDM machining of highly distorted closed surfaces. This approach utilizes a discrete point trajectory planning technique to determine the optimal position and orientation of the electrode. A specialized dataset, generated using the Monte Carlo method in combination with Arena's Principle, is used to train an artificial neural network (ANN), ensuring an efficient and user-friendly optimization process. The optimization model developed for a shrouded blisk focuses on multiple objectives, such as minimizing iteration count, reducing axial motion, and improving machining surface quality. Experimental results show a 17.38% reduction in machining cycle time, along with increased consistency and precision in surface roughness and profile accuracy compared to conventional methods.

EDM Tools underwent development for many years due to poor machining stability, which prevented the tooling's machining stability. EDM Tools gained a surge of excitement when a development of EDM Tools' adaptive control system is presented. An innovative design for addressing this problem has led to the establishment of intelligent EDM, an innovative approach for electrical discharge machining, which has been suggested by Reference [10]. Smart EDM operates with three main functions: first, perception, which measures the gap between the electrode and the workpiece, but only after receiving discharging pulses; second, cognition, This integrates the "gap environment" index and the machining state index, offering guidance for future actions., and third, decision-making, which

involves determining control laws based on the information acquired through perception and cognition.

The use of EDM in manufacturing, particularly for gap flushing, has been described in Reference [11] as Acoustic Immersion (AE), due to its capability to withstand gaps and detect metallic debris and gas bubbles. The local medium where single discharges occur, and through which the AE is extrapolated, holds valuable process information about the efficiency of material removal at the scale of individual discharges. Multiple factors [12] can be used to assess the effectiveness of the EDM process. In addition to the component quality, which is influenced by the cutting rate, the cutting rate itself plays a crucial role in determining the performance of the primary cut. Process stability is another key factor in evaluating the overall process performance. Various studies have been conducted to identify wire breakage by analyzing discharge distribution to predict potential issues.

The Reference [13] noted that EDM and PECM were employed by to machine various materials through an engineered mix of high-speed DCM and low-speed PECM. EDM has the potential to produce materials in machines with electrically higher than a minimum electrical conductivity, but with some tool wear and heat increase. PECM doesn't have as many capabilities to machine materials that form a passive layer or contain chemically soluble contents, making it a challenging process to produce, especially in low-temperature PECM, due to its limited capabilities. The process chain can be structured to involve copper electrodes being assembled by PECM and later used for EDM in an EDM process.

In order to create electrically conductive materials that are extremely hard, machining techniques called electrical discharge machining are utilized, particularly for very hard materials, The cutting parameter used in the electrical discharge machining procedure is mainly dependent on the surface roughness ( $R_a$ ) of the cutting device. A mathematical model is to be created by developing a response graph modeling (RGM), with the reference point being Reference research [14], Utilizing a CNC-EDM machine to cut 304 steel with a dielectric solution of gas oil while applying DC current values of 10A, 20A, and 30A., the impact of various parameters on the surface roughness of the material was evaluated. The findings are significant for reducing the time and cost of predicting surface roughness ( $R_a$ ) in industrial applications.

The alteration of microstructures and changes in mechanical properties of AISI 444 stainless steel structures is explored by examining the impact of gradient fraction in HAZ on the mechanical properties of the structure. In this research, Heat Affected Zone (HAZ) with two types of voltage (140, 240)V to define the effect of voltage

value on mechanical properties. The gap in knowledge that this research is necessary to explain the relation between the power types with Heat Affected Zone. The research results formulated the theory that it is more likely to be able to obtain solid-state samples with high strength through the results.

## 2. HEAT AFFECTED ZONE (HAZ)

The weld where the solid base metal on both sides of the welding element absorbs heat energy from the welding heat cycle alters its structure and properties is referred to as the heat-affected zone, A welded joint is a welding process that involves three parts: the weld seam, the fusion zone, and the heat-affected zone as illustrated in Fig.1, A Heat Affect Zone is the region within the welds on both sides of the weld where the structure and properties experience significant changes, typically within a specific temperature range or at a rate consistent with a fusion connecting temperature, and is known as the Heat Affect Zone. Scientists in various countries have been researching and analyzing the insula, or areas of heat consumption, for decades., The constant use of various materials in manufacturing, including high-strength steels, stainless steels, heat-resistant steels, and some special materials, has caused the joints' weak area to become a more complicated and intricate issue than the previously mentioned heat-affected zone [15].

Thermal conductivity, which is dependent on the amount of energy in a region with high heat intensity, determines the extent of thermal damage. The duration of the HAZ extension depends on various factors such as the quantity of heat used, The HAZ factor in a process can be affected by the temporal complexity of the exposure, material characteristics, and the time period of the exposure, resulting in a smaller HAZ when cooled at a faster rate than with low heat input; whereas, a process with higher heat input will have a slower cooling rate and an effect on the HAZ factor for the same material. Material with HAZ may not adhere to a specific method or cutting method, as it has a different impact on the cutting process compared to materials not impacted by a specific method or cutting process. The internal HAZ in plasma cutting is caused by a higher HAZ in current cutting, and the currents in plasma cut with higher currents result in a narrower HAZ, while oxyacetylene cutting has a wider HAZ due to the combination of high heat, slow speed, and flame width [16]. Electrical Discharge Machining (EDM) is an advanced metal cutting technique that operates on the principle of minimal tool force during machining. It is particularly

effective for processing extremely hard, electrically conductive materials. One of the most critical parameters in EDM is surface roughness (Ra). Traditional trial-and-error approaches to optimizing this parameter are often inefficient, consuming both time and resources.

This research aims to develop a mathematical model using Response Graph Modeling (RGM) to enhance optimization. The study examines the impact of key parameters, including current, pulse-on time, and pulse-off time, on surface roughness. A total of 27 samples were processed using a CNC-EDM machine to cut 304 steel with a gas oil dielectric solution. The machining process was conducted at a voltage of 140V, utilizing DC current values of 10A, 20A, and 30A. A copper electrode was employed to cut through 1.7mm thick steel.

The findings of this research offer significant industrial benefits by reducing both the cost and time required for surface roughness (Ra) prediction. Analysis of the response graph and response table reveals that current and pulse-on time have the most substantial influence on surface roughness, whereas pulse-off time has a negligible impact. Across 27 experiments, the highest recorded surface roughness was 4.22  $\mu\text{m}$ , while the lowest was 2.02  $\mu\text{m}$ . Qualitative results indicate a direct correlation between increasing current and pulse-on time and higher surface roughness values.

The long-term improvement of Ti64 corrosion resistance can be achieved through the use of an EDM process that boosts the material's long-lasting impact. The corrosion of Ti-6Al-4V (Ti64) in simulated body fluid (SBF) is investigated in a reference study using different bath compositions (oil, water, and hydroxyapatite dissolution (HA) after EDM treatment. The corrosion mechanisms were analyzed through immersion periods ranging from 2 h to 3 months, using both electrochemical and microscopy techniques to determine their longevity. Research revealed that EDM-treated samples treated with water demonstrated the highest corrosion resistance, while those treated with oil had the lowest.

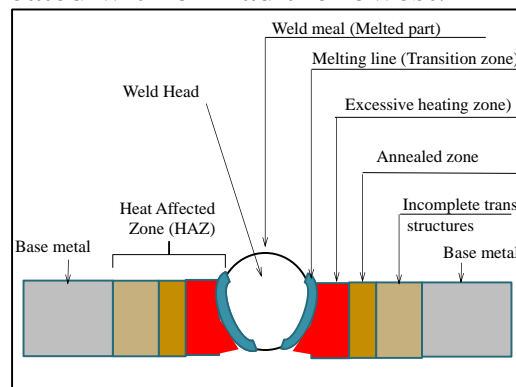


### Figure 1-Schematic of Heat Affected Zone (HAZ)

This study has compared the effects of different voltages on the outcomes of powers and the efficiency of the cutting process by defining the consequences of their changes in various types of voltages.

## 3- EXPERIMENTAL TEST

### 3.1 Experimental work

This work focuses on the use of an extruded AISI 444 stainless steel in temper condition T6, which is the basic material investigated in this work. Table 1 illustrates the chemical composition of the alloy, In the current research published today. Using CNC-EDM equipment, steel 304 was cut with a dielectric solution of gas oil by applying DC current values of 10A, 22A, and 50A. A total of 27 samples were produced. The machining process employed electric currents of 140V and 240V to cut 1mm thick steel, utilizing a copper electrode. The empirical tests were conducted using a CHEMER EDM machine (CM 323C) at the Machine Tool Laboratory, University of Technology. As illustrated in Fig. 2, the experimental setup was designed to ensure precise execution and applicability.

The empirical test was performed using a CHEMER EDM machine (CM 323C) in the Machine Tool Laboratory at the University of Technology, as illustrated in Fig. 1. The workpiece used in this study measured 40×30×1.7 mm and was made of stainless steel (SS) 304, ASTM A 240. The chemical composition of the SS 304 workpiece material was analyzed in the laboratories of the State Company for Inspection and Engineering Rehabilitation, with the results detailed in Table 1. Additionally, the mechanical and physical properties of SS 304 are provided in Table 2. A copper tool with 99.74% purity and a 5 mm diameter was used in conjunction with a gas oil dielectric solution.



Figure 2. -Electro discharge machine (EDM) Model (CM 323C).

### 3.2 Experimental Part

This study aims to examine the effects of EDM machining parameters on the Heat-Affected Zone (HAZ) of an AISI 444 stainless steel workpiece using a copper electrode and a gas oil dielectric solution. Table 1 shows the Chemical composition of AISI 444 stainless steel. The machining process utilizes DC current and low voltage levels (140V and 240V) to cut a 1mm thick workpiece. A second-order Response Graph Modeling (RGM) approach is employed to develop a mathematical model based on the experimental findings.

**Table 1. - Chemical composition of AISI 444 stainless steel.**

Element	C	Si	Mn	P	S	Cr
Weight %	0.0237	0.340	0.206	0.0247	< 0.0005	19.08
Element	Ti	Al	Cu	Ni	Mo	Fe
Weight %	0.237	0.0056	0.121	0.252	< 0.002	Bal.

Table 2 presents the experimental results for all voltage values. Additionally, the EDM method was employed to optimize machining conditions using Response Graph Modeling (RGM) to determine the most influential input parameters affecting the output response during the cutting process.

**Table 2. - Fixed parameters of the EDM machine.**

Machining parameters	Work-piece polarity	Electrode polarity	Dielectric fluid	S code
Fixed values	Negative	Positive	Transformer oil	20

Gap code	Jumping Time	Servo feed	Working Time	Depth of cut
9	0.8 s	0.75	0.6 s	1 mm

**Table 3 - Machining parameters and it's levels.**

Parameters	Units	Levels		
		Level 2		Level 3
Voltage	V	140	240	50
Peak current ( $I_p$ )	A	12	24	
Pulse on time ( $T_{on}$ )	$\mu s$	100	200	400
Pulse off time ( $T_{off}$ )	$\mu s$	6.5	3	12

Table 4 provides the experimental results for all voltage values, highlighting the most influential input parameters for each output response in the cutting process.

**Table 4 - The experiment results of Heat Affected Zone (HAZ).**

No. of sample	Current $I_p$ (A)	Pulse on $T_{on}$ ( $\mu s$ )	Pulse off $T_{off}$ ( $\mu s$ )	HAZ ( $\mu m$ )	
				140 (V)	240 (V)
1	12	100	3	5.486	8.202
2	12	100	6.5	5.582	8.314
3	12	100	12	5.62	8.326
4	12	200	3	5.746	8.342
5	12	200	6.5	5.756	8.364
6	12	200	12	5.786	8.414
7	12	400	3	6.344	8.431

8	12	400	6.5	6.414	8.464
9	12	400	12	6.464	8.476
10	24	100	3	12.468	17.115
11	24	100	6.5	12.525	17.133
12	24	100	12	12.549	17.154
13	24	200	3	12.615	17.496
14	24	200	6.5	12.693	17.523
15	24	200	12	12.732	17.553
16	24	400	3	12.759	17.763
17	24	400	6.5	12.783	17.919
18	24	400	12	12.825	18.045
19	50	100	3	28.048	32.971
20	50	100	6.5	28.604	33.079
21	50	100	12	28.692	33.147
22	50	200	3	28.783	33.412
23	50	200	6.5	28.932	33.984
24	50	200	12	29.016	34.798
25	50	400	3	29.444	34.825
26	50	400	6.5	29.526	35.649
27	50	400	12	30.272	36.679

#### 4. RESULTES AND DISCUSSION

The graph below illustrates the direct proportional relationship between the HAZ and sample number, with the highest possible reading (HAZ) for 27 samples determined from 27 samples and the lowest possible number indicating 140V. The same pattern is observed when the voltage is raised to 240v, indicating a similar proportion 3 times, The compacted data set in Fig 2, demonstrates two cases of voltages differing from each other, experimental validation by stating that the Heat Affected Zone (HAZ) increased as the voltages values increased. The number 4 was

used to inform the group that a higher voltage level meant an increase in the Heat Affected Zone (HAZ) without more voltage.

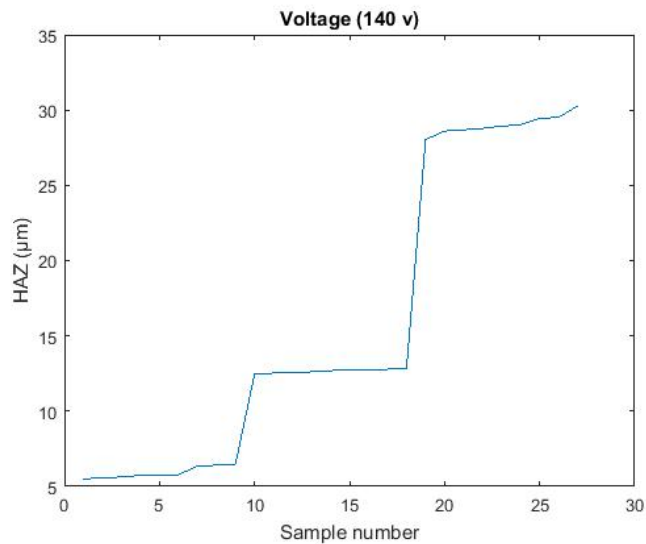


Figure 3. -Relationship between the HAZ and sample number for 27 samples and 140V.

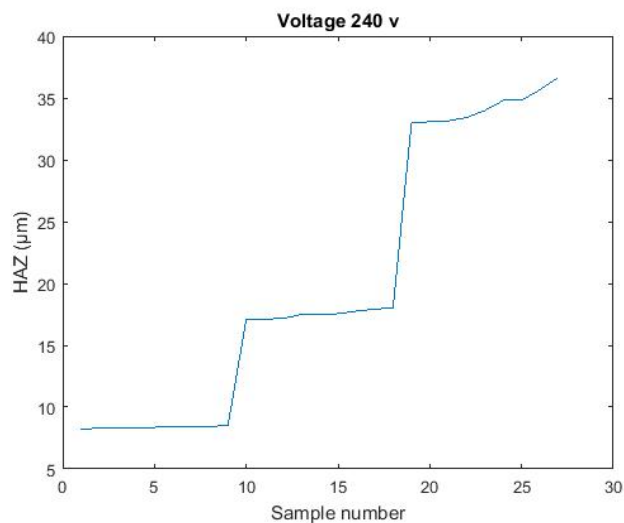


Figure 4 -Relationship between the HAZ and sample number for 27 samples and 240V.

The figure demonstrates that the Heat Affected Zone (HAZ) increases with changes in voltage (V) from 140V to 240V and current (Ip) from 12A to 50A. As voltage increases, there are more electron collisions and stronger sparks, which raise the temperature between the electrode and the workpiece. This result in melting, vaporization, and the formation of larger craters on the surface of the workpiece material. The HAZ also increases as the pulse-on time (Ton) rises from 100 to 400

microseconds, as this allows more energy to be discharged through the plasma channel, with a longer conversion time into the electrode. Conversely, HAZ decreases as the pulse-off time ( $T_{off}$ ) increases from 3 to 12 seconds, as the spark discharge time and intensity are shortened, narrowing the plasma channel and reducing the impact of electrons on the workpiece.

However, some values may not align with predictions due to external factors like energy depletion, machine vibrations, or dielectric contamination. The maximum material removal rate (MRR) is observed at  $T_{off} = 6.5$  seconds, with optimal results achieved at 240V,  $I_p = 50A$ , and  $T_{on} = 400$  microseconds. The MRR can also reach its maximum with variations of  $T_{off} = 6.5$  microseconds, and values of 240V and  $T_{on} = 100$  microseconds are also effective for achieving high MRR.

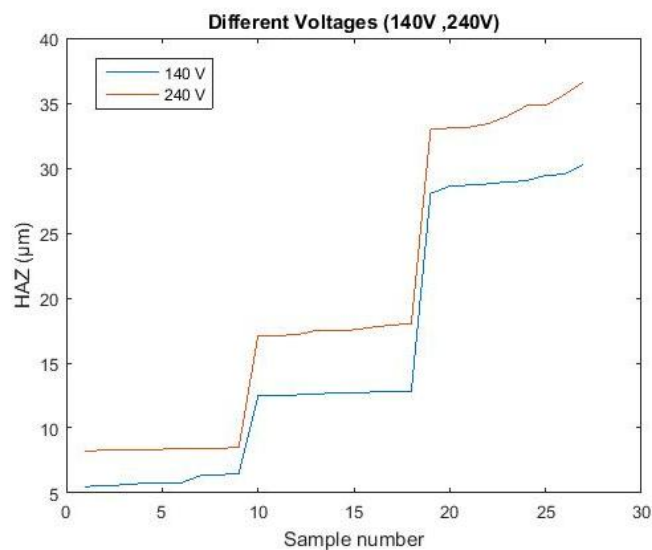


Figure 5 -Relationship between the HAZ and sample number for both voltages (140. 240V).

This study considered the following parameters: voltage (140V, 240V), current ( $I_p$ ) (12A, 24A, 50A), pulse-on time ( $T_{on}$ ) (100 $\mu$ s, 200  $\mu$ s, 400  $\mu$ s), and pulse-off time ( $T_{off}$ ) (3  $\mu$ s, 6.5  $\mu$ s, 12  $\mu$ s). The Heat Affected Zone (HAZ) was examined under these conditions, with the same parameters used experimentally, as described above. The copper electrode was utilized in the tool during the process. The quality of the machined surface is influenced by the voltage value applied in the EDM process, with different voltages affecting the outcome. Specifically, the HAZ under 240V is more distinct and measurable than the HAZ under 140V.

## 5. CORRELATION COEFFICIENT VALUES

## 5.1 Definition of Correlation Coefficient Values

When two variables are correlated, they indicate how strong a relationship tends to be between them; an arithmetic coefficient is used to determine this relationship. Correlation coefficient values usually lie within the range of -1 to 1, with a range of 0-1. If the correlation coefficient of a correlation is 1, then the increase in one variable is positive for every positive increase in the other, implying a positive increase in the other. Zero implies that there is no change in the value of every increase, i.e., zero means that no increase is positive or negative. The two are not intertwined as evidenced by Fig.6.

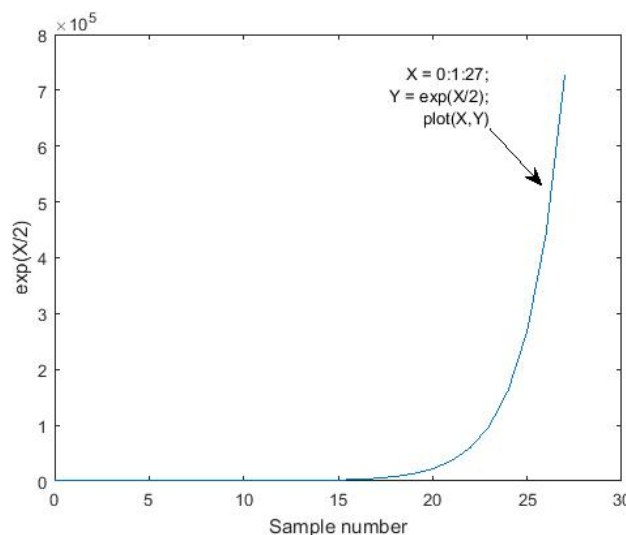


Figure 6 -Graph presenting a correlation coefficient of  $(\exp(x/2))$ .

## 5.2 Correlation Coefficient Values and HAZ

An association is measured through the presence or absence of information, which is then quantified by a correlation coefficient. The particular interest was the relationship between the HAZ value obtained from the structural parameters of the 140V and 240 voltages and their practical applications, with regard to sensitivity, sensitivity, and elastin content. In the same way as shown in Fig. 5 illustrates that the correlation coefficient between the curve of HAZ and  $(\exp(x/2))$  when the voltage is 140V and voltage is 140V is 0.5913 with each curve, Despite the voltage being 240V shown in Fig.7, it is estimated to be 0.6022 when the voltage is 240V as in Fig 8.

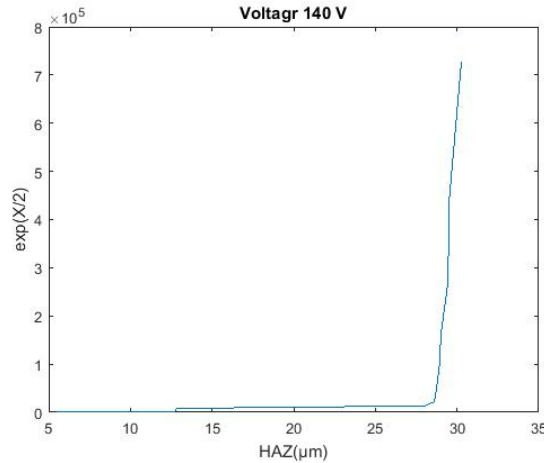


Figure 7 - Relationship between the HAZ and Reciprocal function ( $\exp (x/2)$ ), when 140V.

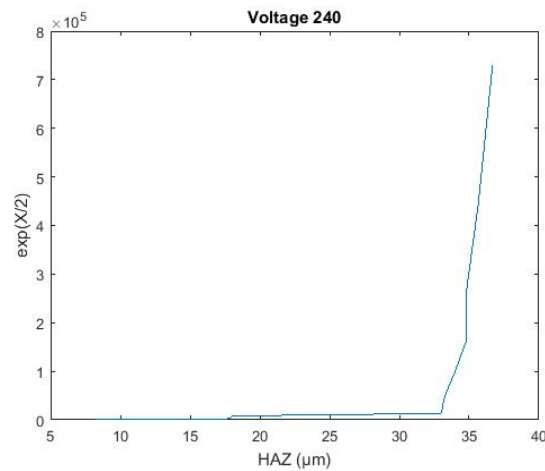


Figure 8- Relationship between the HAZ and Reciprocal function ( $\exp (x/2)$ ), when 240V.

## 6. FINDINGS

The research aimed to utilize a wear model for EDM electrodes to predict cutting depth and analyze the morphology of copper electrodes after processing. The study focused on the machining of AISI 444 stainless steel alloy, which was subjected to heat treatments to observe the heat-affected area (HAZ) in a welded connection during the machining process. Both experimental and numerical methods were incorporated, with the numerical part involving real heat treatments and tension testing. The effects of low and high strain rates on strength, strain-rate sensitivity, and fracture were tested, using various tests to assess damage caused by additional

heat treatments. The numerical section of the study analyzed two commonly used machining models, with voltages of 140V and 240V. The significance of machining parameters in an idealized HAZ, under these two voltages, was highlighted through a case study. It was found that the HAZ weakens as the Toff (pulse-off) time increases, with the highest HAZ observed at Toff = 12  $\mu\text{m}$  for the conditions: voltage 240V, current  $I_p = 50\text{A}$ , and  $T_{on} = 400 \mu\text{m}$ . On the other hand, the lowest HAZ values were measured at Toff = 12  $\mu\text{m}$ , voltage 140V, current  $I_p = 12\text{A}$ , and  $T_{on} = 400 \mu\text{m}$ . The correlation coefficient for the relationship between HAZ and the reciprocal function was found to be 0.5913 and 0.6022, respective.

**REFERENCES**

- [1] P. G. Hess, L. Heidemanns, T. Herrig, A. Klink, and T. Bergs, "Simulation based derivation of changed rim zone properties caused by thermal loadings during EDM process," *\*Procedia CIRP\**, vol. 113, pp. 41-46, 2022.
- [2] P. Steuer, A. Rebschläger, O. Weber, and D. Bähre, "The Heat-affected Zone in EDM and its Influence on a Following PECM Proc," *\*Procedia CIRP\**, vol. 13, pp. 276-281, 2024.
- [3] H. a, L. Heidemanns a, T. Herrig a, A. Klink a, and T. Bergs a b, "Model Based Prediction of the Heat Affected Zone in a Steel Workpiece Induced by an EDM Single Discharge," *\*Procedia CIRP\**, vol. 117, pp. 263-268, 2023.
- [4] V. V. Lyubimov, V. M. Volgin, I. V. Gnidina, and M. S. Salomatnikov, "Formation of the Workpiece Shape and Surface Finish During Electrical Discharge Machining," *\*Procedia CIRP\**, vol. 68, pp. 319-324, 2018.
- [5] N. Ahmed, "Machining and wear rates in EDM of D2 steel: A comparative study of electrode designs and materials," *\*Journal of Materials Research and Technology\**, vol. 30, pp. 1978-1991, 2024.
- [6] S. Arun, M. Manikandan, J. Joshy, B. Kuriachen, and J. Mathew, "Numerical modelling and experimental investigations to predict the tool wear of copper electrodes during  $\mu$ -EDM process," *\*CIRP Journal of Manufacturing Science and Technology\**, vol. 55, pp. 174-187, 2024.
- [7] K. Saxena, V. Volski, J. Qian, G. Vandenbosch, and D. Reynae, "On-machine evaluation of micro-EDM process signature in radio frequency (RF) domain: A step towards cost-effective data collection in a multiphysical process," *\*Journal of Materials Processing Technology\**, vol. 335, p. 118663, 2025.
- [8] H. Farooq and R. A. Pasha, "Investigation of process parameters for modeling of ceramic composite SiSiC IN dry EDM (DEDM cutting," *\*Heliyon\**, vol. 10, no. 17, p. e36459, 2024.
- [9] Z. Wang, X. He, X. Geng, C. Guo, B. Xu a, and F. Gong, "Novel machine learning-driven multi-objective optimization method for EDM trajectory

- planning of distorted closed surfaces," *\*Precision Engineering\**, vol. 90, pp. 141-155, 2024.
- [10] X. Mu, M. Zhou, J. Zhang, N. Lu, and Q. Ye, "Intelligent electrical discharge machining (EDM) molybdenumtitaniumzirconium alloy by an extended adaptive control system," *\*Journal of Manufacturing Processes\**, vol. 77, pp. 207-218, 2022.
- [11] A. Goodlet and P. Koshy, "Real-time evaluation of gap flushing in electrical discharge machining," *\*CIRP Annals\**, vol. 64, no. 1, pp. 241-244, 2015.
- [12] IU. Küpper, T. Herrig, A. Klink, D. Welling, and T. Bergs, "Evaluation of the Process Performance in Wire EDM Based on an Online Process Monitoring System," *\*Procedia CIRP\**, vol. 95, pp. 360-365, 2020.
- [13] P. Steuer a b, A. Rebschläger a, O. Weber b, and D. Bähre, "The Heat-affected Zone in EDM and its Influence on a Following PECM Process," *\*Procedia CIRP\**, vol. 13, pp. 276-281, 2014.
- [14] S. H. Aghdeab, N. Hafidh, and M. Q. Ibraheem, "Surface Roughness Prediction for Steel 304 In Edm Using Response Graph Modeling," *\*Al-Khwarizmi Engineering Journal\**, vol. 14, no. 4, pp. 115-12, 2018.
- [15] "What is the welding heat-affected zone?" [Online]. Available: [<https://www.harsle.com/what-is-the-welding-heat-affected-zone?srsltid=Af>](<https://www.harsle.com/what-is-the-welding-heat-affected-zone?srsltid=Af>). [Accessed: Apr. 22, 2025].
- [16] "What is the heat-affected zone?" [Online]. Available: [<https://www.twi-global.com/technical-knowledge/faqs/what-is-the-heat-affected-zone>](<https://www.twi-global.com/technical-knowledge/faqs/what-is-the-heat-affected-zone>). [Accessed: Apr. 22, 2025].
- [17] J. I. Ahuir-Torres a, J. Chadwick b, G. West c, H. R. Kotadia b c, and T. T. Öpöz, "Effect of electrical discharge machining (EDM) bath composition on long-term corrosion of Ti-6Al-4V in simulated body fluid," *\*Electrochimica Acta\**, vol. 503, p. 144865, 2024.
- [18] "Correlation Coefficient Formula," [Online]. Available: [<https://www.statisticshowto.com/probability-and-statistics/correlation-coefficient-formula/#Pearson>](<https://www.statisticshowto.com/probability-and-statistics/correlation-coefficient-formula/#Pearson>). [Accessed: Apr. 22, 2025].